FORMATION MECHANISM AND PROPAGATION CHARACTERISTICS OF THE EQUATORIAL THERMALLY-FORCED SHORT-TERM CLIMATIC OSCILLATION DURING THE NORTHERN SUMMER

Ni Yunqi (倪允琪), *Lin Wuyin* (林武银) and *Li Yaodong* (李耀东)

Department of Atmospheric Sciences, Nanjing University, Nanjing

Received January 2, 1989

ABSTRACT

In this study, in order to investigate the global climatic oscillations forced by sea surface temperature (SST) anomalies over equatorial central-eastern Pacific, two numerical schemes with different SST distributions (normal and anomalous cases) are tested by using a nine-layer global spectral model. Experiment results show that (i) in northern summer, a wave train that is similar to the teleconnection pattern suggested by Nitta (1987) and Huang (1987) in the Northern Hemisphere and another one in the Southern Hemisphere are reproduced; (ii) simulated results suggest that the response of atmosphere in middle-high latitudes of both hemispheres to an anomalous heating source is more sensitive in tropical western Pacific than in equatorial central-eastern Pacific; and (iii) in northern summer, the formation of low-frequency oscillations on monthly (seasonal) time scale results from energy dispersion as well as interactions between eddies and zonal flow, and between eddies.

I. INTRODUCTION

Teleconnection is a very important phenomenon in the atmosphere. It not only reveals that there is a process of remote response in the atmosphere, but also has very important significance for improving the long-range weather prediction or the short-range climatic prediction. The phonomenon and the concept were first found and proposed by Walker and Bliss (1932). Afterwards, observed facts identified existence of the teleconnection phenomenon in the atmosphere (Sawyer, 1970; Van Loon and Rogers, 1978; Wallace and Gutzler, 1981; Blackmon et al., 1983; Mo and White, 1985; Nitta, 1987). These teleconnection patterns are regarded as evidence of the effects of thermal forcing, such as sea surface temperature anomalies (SSTA) and thermal state of land surface on the atmosphere. Especially, attention has commonly been placed on studying the effects of SST on the atmosphere in recent years. Bjerknes (1966) and Rowntree (1972) have studied the effects of SSTA over equatorial Pacific and northern Atlantic on the atmosphere, respectively. Rusmusson and Carpenter (1982) and Blackmon (1983) further insighted into the ENSO phenomenon. The above investigations clearly indicated that equatorial SST has a significant influence on the global climate and general atmospheric circulation, especially the PNA pattern may be produced in the northern winter. Advance in studying the effects of SSTA on the atmosphere has greatly been made by using GCM. Simulated results showed that in the northern winter, a wave train was produced by equatorial SSTA, which bears a resemblance to the PNA teleconnection pattern (Blackmon et al., 1983; Geister et al., 1985). In the southern winter and summer, the remote response was simulated, which basically was in agreement with observations, in the middle and high latitudes (Webster, 1981), while a response which resembles the remote response suggested by Nitta (1987) and Huang (1987) was also simulated in the northern summer (Huang and Wu, 1988).

Theoretical studies indicated that the mechanism of the above teleconnection patterns may be either dispersion of two-dimensional Rossby wave resulting from the localized forcing (Hoskins and Kalory, 1981; Horel and Wallace, 1981) or internal dynamic process of the atmosphere (Lau, 1981). Simmons et al. (1983) have explored relationship between propagation of the Rossby waves, barotropic unstable modes of basic flow and atmospheric teleconnection and indicated that the western Pacific and Atlantic areas were sensitive areas of atmospheric response to the external forcing. As a result, the barotropic unstable modes of mean basic flow were developed over these areas and generated the teleconnection patterns.

The generation and propagation mechanisms of the two-dimensional Rossby waves resulting from response of the atmosphere to El Nino are not very clear although the investigations mentioned above indicate that the dynamical processes of atmospheric response to SSTA have been correspondingly understood (Gill, 1980; Webster, 1981; Sadeshmukh and Hoskins, 1985; Held and Kang, 1987). Therefore, the project is worthy of further investigation.

In this paper, in order to study the above problem we attempt to analyze the evolution processes of local and reomte response in the Northern and Southern Hemispheres using the simulated data by Lin and Sun (1987).

A brief description of the model and the experiment schemes is provided in Section II. The simulated teleconnections in the Northern and Southern Hemispheres are detailed in Section III. The evolution processes of the local and remote responses are given in Section IV. The formation and propagation mechanisms of the waves are discussed in Section V, and summary and conciusions in Section VI.

II. BRIEF DESCRIPTION OF THE MODEL AND EXPERIMENT SCHEMES

A detailed description of the global model used in this study and the assessment of its simulation capability can be found in McAvancy and Bourke (1978). The model is only briefly described in this paper.

The basic dynamic and thermodynamic equations of the model consist of horizontal divergence equation, vorticity equation, the tendency equation of logarithmal surface pressure, thermodynamic equation, the moisture tendency equation, and diagnostic equations for vertical velocity and the hydrostatic relationship. Cast on spherical coordinate in the horizontal and sigma coordinate in the vertical, these equations are solved by using the Galerkin procedure when model variables are represented as truncated expansion of spherical harmonics with rohmbodal truncation at wavenumber 15. The model makes use of the semi-implicit time integration scheme with a time step of 30 min.

In the model, the physical processes and parameterizations include short-wave radiation, long-wave radiation, large-scale condensation and convection, vertical diffusions of momentum, heat and moisture and the effects of underlying surface (including ocean, polar ice and snow cover) and topography on the model atmosphere are considered.

In order to investigate the formation mechanism and the propagation characteristics of the short-range climatic oscillation forced by SSTA over the equatorial Pacific during the El Nino period, two different experiment schemes are tested and compared each other:

Scheme 1, control case (hereinafter referred to as Exp 1). SST used in the model is climatological mean values in July and CO_2, O_3, snow cover and polar ice coverage are also climatological mean values in July and sun's altitude angles in mid-July are used.

Scheme 2, anomalous case (hereinafter referred to as Exp 2). SST used in the model is the idealized SSTA field similar to observed SSTA over eastern Pacific (shown in Fig. 1, Lin and Sun, 1987), superposed upon the climatological mean SST field in July. The maximum SSTA is 4.4°C. Others in the model are same as Exp 1.

The model was spun up with perpetual July boundary conditions and forcing starting with a rest atmosphere and integrated for 492 days. Then the two schemes are continuously run for 40 days with simulation at Day 492 as initialization and the July monthly average simulated results are obtained from the last 30 - day averaged simulations of two experiments, respectively.

III. MONTHLY (SEASONAL) RESPONSE OF ATMOSPHERE TO EL NINO IN NORTHERN AND SOUTHERN HEMISPHERES

Fig. 1a and Fig. 1b represent the monthly averaged geopotential height difference between Exp 2 and Exp 1 simulations at 300 hPa and 850 hPa in July, respectively. Comparison of Fig. 1a with Fig. 1b shows that the response of atmosphere to equatorial SSTA in the Southern Hemisphere (winter hemisphere) is stronger than that in the Northern Hemisphere (summer hemisphere). Furthermore, the response of atmosphere is more evident in areas where are farther away from the heat source in both hemispheres. Fig. 1 also shows that not only strong remote response exists in the winter hemisphere, but also there is apparent remote response in the middle-high latitudes of the summer hemisphere. These results are in disagreement with Webster (1982), who suggested that the response in middle-high latitudes of the summer hemisphere was weak, but analogous to the simulation with SSTA over equatorial central and eastern Pacific by Keshavamurty (1982).

A comparison between upper and lower atmospheric responses to the equatorial heat source shows that there are a pair of positive geopotential difference response on both northwest and southeast sides of the SSTA area at 300 hPa and a pair of negative geopotential difference response on west side of the equatorial heat source at 850 hPa. However, the remote response to the north of subtropic zone far away from the heat source is in phase between upper and lower troposphere in both hemispheres, which sheds much light upon the equivalent barotropic structure. The above results show the local response and remote response in the model atmosphere comparatively agree with theoretical results (Gill, 1980; Webster, 1981, 1982; Lau et al., 1984).

The observed geopotential height anomalies of the northern hemisphere at 500 hPa in July, 1972 are given in Fig. 1c. Comparing Fig. 1a with Fig. 1c indicates that the negative anomaly area over South China and the tropical western Pacific and the positive anomaly area over Japan and Northeast China are simulated although in contrast, the simulated positive area is extended further westward compared with the observed in Fig. 1c. However, the observed precipitation anomaly map (not shown) shows that the negative precipitation anomaly area is located in the belts along the Changjiang and the Huanghe Rivers, which corresponds to the distribution of simulated geopotential height differences. In Fig. 1c, a strong positive anomaly area exists over northeastern Asia, Alaska and the east coast of North America, and the positive difference area corresponding to the above positive anomaly area in the simulated geopotential height difference at 300 hPa can be found. The observed facts, i. e., the positive anomaly areas are over Europe and central-north Africa, the negative anomaly areas are over Mediterranean Sea and neighbourhood and the central Canada, and the positive anomaly area to the southeast of the negative area are over the central Canada, are reproduced in the model (see Fig. 1a). However, the centers of the simulated negative area over northeastern Asia and the simulated positive area over North America are located further west compared with observations. The reason why this discrepancy is given rise to so far is not clear. The point to stress is that up to now, the general circulation models have probably been behaving in a manner consistent with the above discrepancy in the light of simulations. It is noteworthy that the resemblance of alternating the positive and the negative difference areas between simulations and observations in the Northern Hemisphere is suggestive of a wave train propagating northward from the tropical western Pacific. This result is in agreement with the teleconnection in summer of the Northern Hemisphere found by Nitta (1987) and Huang (1987). Furthermore, the negative center located over bound of Canada and eastern United States existing in both simulations and observations might be viewed as the fifth activity center of the above wave train. The correspondance between

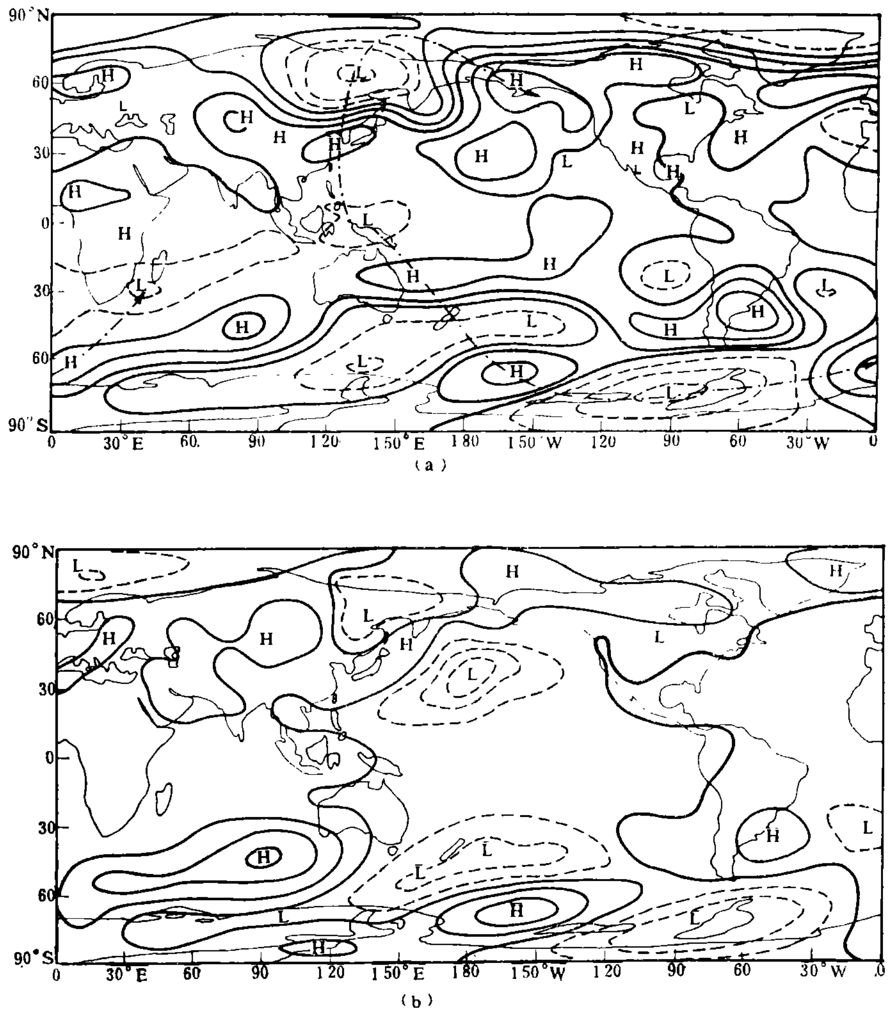

Fig. 1. Simulated July mean geopotential height difference map (Exp 2 minus Exp 1) at 300 hPa (a) and 850 hPa (b).

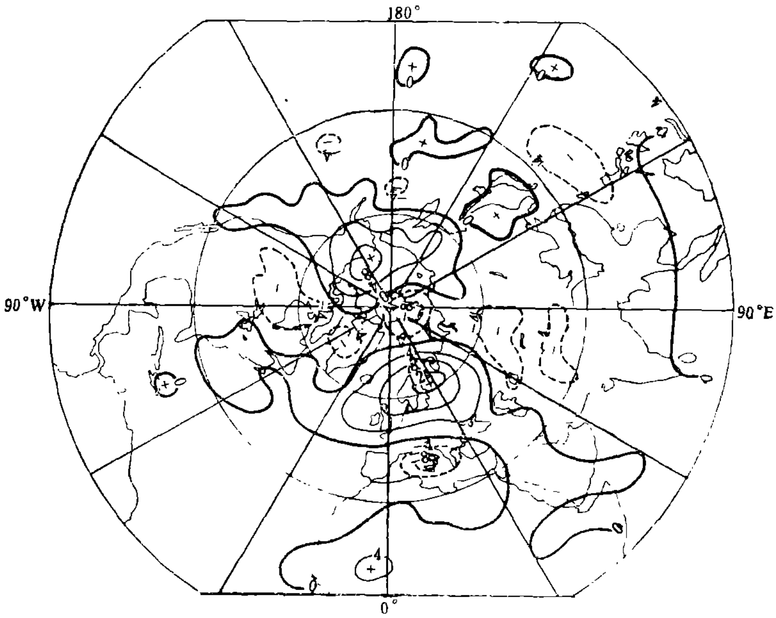

Fig. 1c. Observed geopotential height anomaly at 500 hPa in the Northern Hemisphere in July, 1972 (units: 10 m; internal: 40 m).

the geopotential height difference mentioned above and precipitation difference is also clear evidence of existence of the above wave train (not shown). It is with this dilemma in mind how to check the simulation in the Southern Hemisphere because of lack of observation data. Fortunately, Ramage (1975) analyzed the stream function anomaly field at 700 hPa and 200 hPa over tropics and subtropics in summer, 1972. Therefore, the simulated results in tropics and subtropics might be compared with Ramage (1975) while simulation in middle-high latitudes can only be compared with simulated results by Webster (1982) and Keshavamurty (1981).

Fig. 1a shows that in the Southern Hemisphere, a wave-train with wavenumber 3 propagates southeastward from a negative difference center over equatorial western Pacific, and then turns northeastward. Its difference centers are respectively located over equatorial central Pacific, south of Southern Pacific, the South Pole region, central South Indian Ocean and north of South Indian Ocean. Extension of each positive or negative member of the wave-train in east-west direction is much longer than that in south-north direction. Therefore, the long axis exhibits a northeast-southwest orientation. The distribution of the geopotential height difference in either the upper or lower troposphere mentioned above agrees with the simulated results by Webster (1982) and Kesavamurty (1981), and simulation in tropics and subtropics is basically analogous to analysis by Ramage (1975).

According to activity center position of the wave train in the Southern Hemisphere, it is seen that the Mascarene high is situated in the last negative difference region whereas the Austrlia high is situated in the first positive difference region. The former weakens the Mascarene high, resulting in weakening the Somali jet; while the latter strengthens the Australia high, resulting in strengthening the cross equatorial flow at 110°E (Ni et al., 1989). The above results show that response of atmosphere in the Southern Hemisphere to El Nino not only causes anomalous general circulation and precipitation, especially the increase of rainfall in Brazil, but also it has an important influence on atmospheric circulation in the Northern Hemisphere via the thermally forced wave train in the Southern Hemisphere, especially summer Asian circulation.

Overall, in northern summer, the wave train propagating eastward from the west coast of Pacific in the Eastern Hemisphere to the east coast of Pacific in the Western Hemisphere plays an important role in the change of atmospheric circulation over East Asia and North America in the Northern Hemisphere, and in the Southern Hemisphere another wave train propagating southeastward from tropical western Pacific, through South Pacific and South Atlantic then entering the Indian Ocean has an evident influence on not only circulation and precipitation of the Southern Hemisphere, but also circulation of the Northern Hemisphere, especially summer Asian circulation due to the monthly (seasonal) response of atmosphere in Northern and Southern Hemispheres to El Nino.

IV. PROPAGATION CHARACTERISTICS OF THE EQUATORIAL THERMALLY FORCED SHORT-RANGE CLIMATE OSCILLATION DURING NORTHERN SUMMER

Figs. 2a and 2b represent the simulated geopotential height difference at 300 hPa on Day 2 and Day 8, respectively.

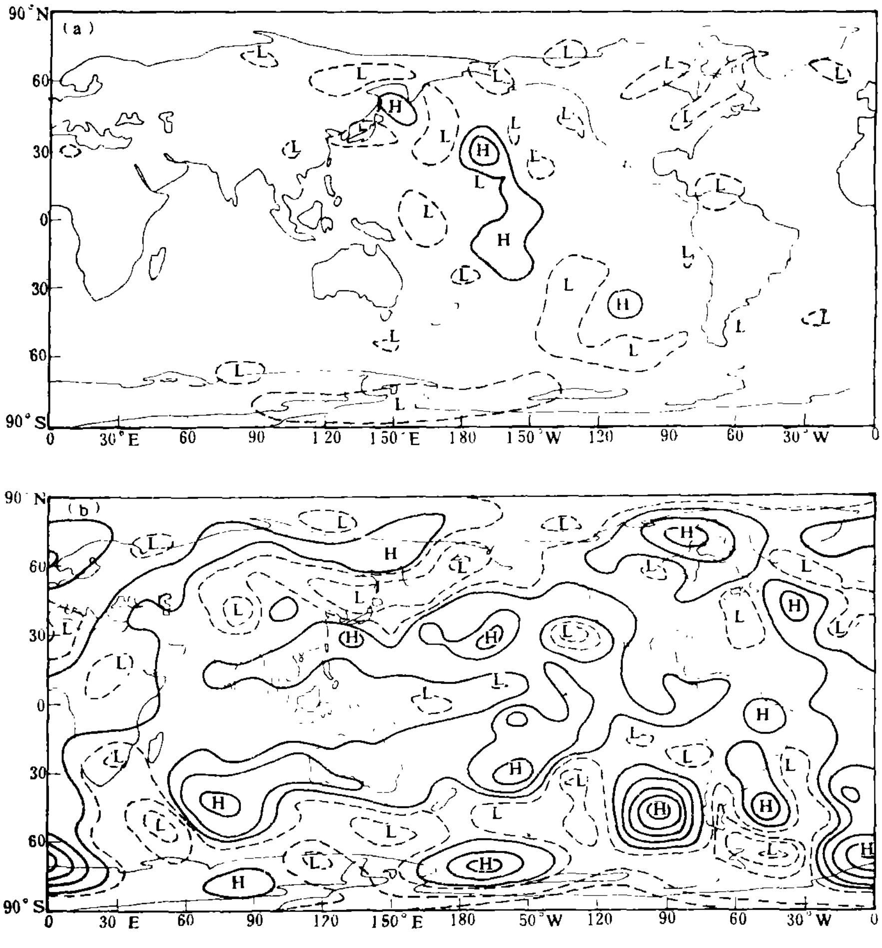

Fig. 2. Simulated 300 hPa geopotential height difference map on Day 2 (a) and Day 8 (b).

Fig. 2a shows that there is a positive center (a negative center at 850 hPa) to the northwest of the heat source in the Northern Hemisphere and another positive center (a negative center at 850 hPa) to the southwest of the heat source in the Southern Hemisphere at 300 hPa on Day 2. Obviously, these difference centers result from baroclinic response of the atmosphere to the heat source at equator (Gill, 1980; Webster, 1981). It is noteworthy that the response is asymmetric about the equator, and the response to northwest of the heat source in the lower is stronger than that in the upper in the Northern Hemisphere and the reverse of this happens in the Southern Hemisphere. The response in the flow field is analogous to that in the geopotential height field (not shown).

In the upper troposphere on Day 4 (not shown), a wave train with four activity centers starting from the positive center near the equator and propagating northwestward is apparently generated. It is interesting to note that a negative center exists in the upper over equatorial western Pacific. Obviously, anomalous SST weakens the Walker circulation resulting in weakening convection activities over tropical western Pacific. Therefore, a positive difference center in the lower and a negative in the upper are generated. Similarly, a wave train propagating southeastward is formed in the Southern Hemisphere. Two wave trains in the lower as same as those in the upper exist in both hemispheres. They exhibit equivalent-barotropic structure in the middle-high latitudes (not shown).

On Day 6 (not shown), the two wave-trains continuously propagate northeastward then return toward southeast and southwestward then return toward northeast, respectively, and new activity centers are formed. It is noteworthy that another wave train is propagating northward from tropical western Pacific when the wave train to northwest of the heat source is formed in the Northern Hemisphere. Member phases of the former are same as the latter apart from the source region. Obviously, this is the wave train found by Nitta (1987) and Huang (1987), which is forced by anomalous convection activities over tropical western Pacific in summer and propagates along the west coast of Pacific through the polar region into the east coast of Pacific. This wave train is superposed on the northwestward dispersed wave train forced by the heat source in equatorial central-eastern Pacific. As a result, it strengthens intensity of the summer wave-train in the Northern Hemisphere, which is found by Nitta (1987) and Huang (1987).

Integration on Day 8 (Fig. 2b) shows that disturbance members of the northward propagating wave train in the Northern Hemisphere are continuously developing and the positive difference area over central North Pacific is extended westward and the whole western Pacific is occupied by the negative difference. It is interesting to note that the wave train northward propagating from tropical western Pacific is gradually strengthened and dominated in the Northern Hemisphere other than the wave train northwestward propagating from the warm pool in equatorial central-eastern Pacific. These results indicate that propagation direction and activity center position of wave trains in the Northern Hemisphere begin to adjust whereas in the Southern Hemisphere, position of the wave train is relatively stable, in which disturbances are continuously developing and a complete wave train is gradually formed.

On Day 10 (not shown). activity centers of northward and northwestward propagating waves are further combined and developed. It clearly appears to be the summer wave pattern in the Northern Hemisphere, which is similar to that found by Nitta (1987) and Huang (1987). This result clearly suggests that even in summer, the response of atmosphere in mid-high latitudes of the Northern Hemisphere to anomalous convection over tropical

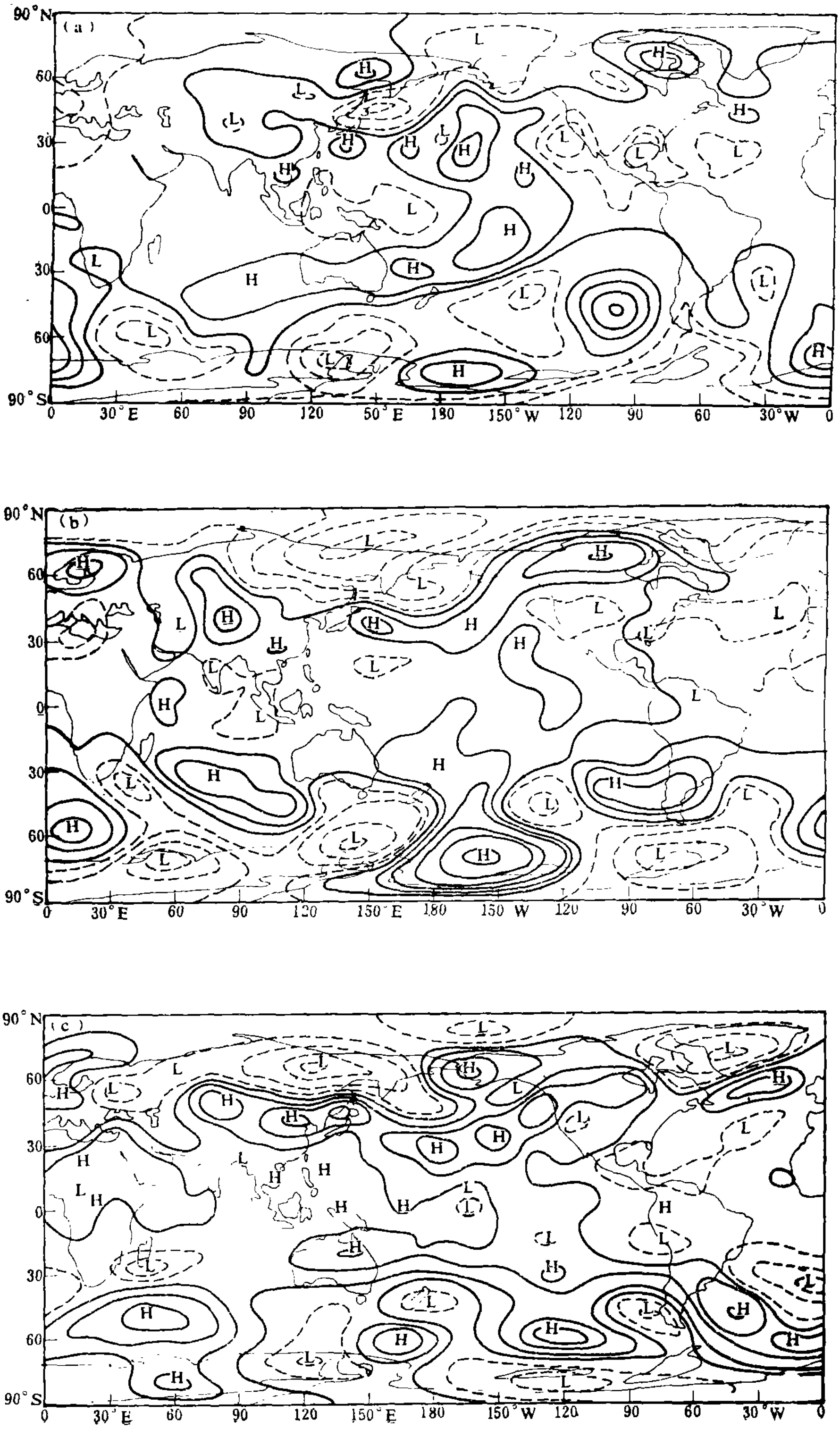
(a)
(b)
(c)
90°N
60
30
0
30
60
90°S
0
30°E
60
90
120
150°E
180
150°W
120
90
60
30°W
0
H
L

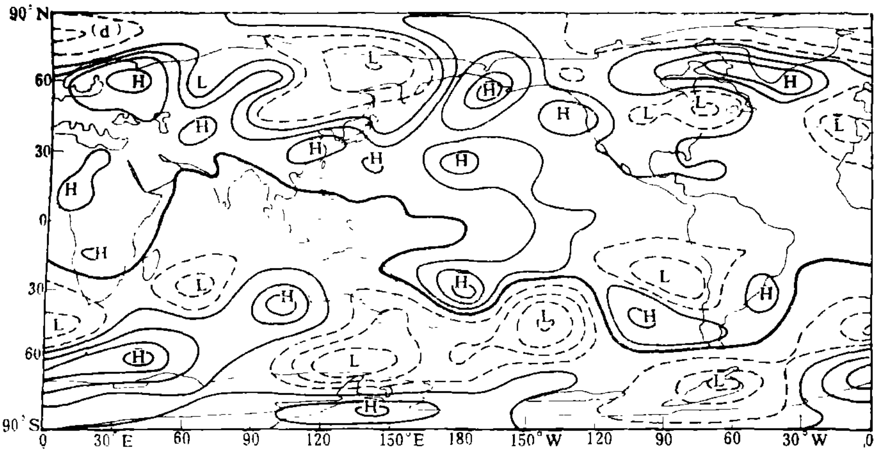

Fig. 3. Five-day averaged geopotential height difference at 300 hPa from simulation: (a) the second five-day average after integration; (b) the fourth five-day average; (c) the sixth five-day average; and (d) the eighth five-day average.

western Pacific is very sensitive and the source region of atmospheric remote response in mid-high latitudes of the Northern Hemisphere seems to be in tropical western Pacific. This result is in agreement with the conclusion suggested by Branstator (1985) who analyzed the mechanism of the remote response in the northern winter. In the Southern Hemisphere, the wave train is developed into the strongest stage with complete structure and wavenumber 4 on Day 10.

Figs. 3a—d represent the second, fourth, sixth and eighth five-day averaged geopotential height differences at 300 hPa, respectively, after the model is integrated.

Fig. 3a indicates that there is a wave train northwestward propagating from northwest of the heat source in equatorial central-eastern Pacific then turning northward through the polar region into the east coast of Pacific and another one northward propagating from tropical western Pacific. Both these two wave trains are combined as a northward propagating wave train over Japan. In winter of the Southern Hemisphere, there is a wave train with wavenumber 3 southeastward propagating from equatorial central Pacific, then entering into South Atlantic and turning toward northeast into the Indian Ocean and almost passing through all the Southern Hemisphere.

In Fig. 3b, it is seen that main members of the wave train located in north of subtropics are moved eastward with a speed of 30m/s once the wave train in the Southern Hemisphere is formed. In contrast to the fourth five-day averaged zonal flow (not shown), it is clear that each member of the wave train is under the control of west wind. Therefore, the disturbances are steered by the westerly. However, the change in position and intensity of the wave-train members with latitudes is due to nonuniform zonal flow. It is noteworthy that there are a pair of positive difference areas (corresponding to negative areas in the lower) to the northeast and the southwest of the heat source in the second five-day averaged difference at 300 hPa. Apparently, this is reflection of baroclinic response of Rossy waves in the upper as mentioned above. However, the positive difference center near the heat source in the Northern Hemisphere disappears and another center in the Southern Hemisphere shifts to the ocean to east of Australia in the fourth five-day averaged difference map. The above facts imply that the source region is likely located in the anomalous convection activity area of tropical western Pacific (weakening of Walker cell results in weakening convection in tropical western Pacific) rather than the heat source region in equatorial central-eastern Pacific in the Southern Hemisphere. A similar variety of the source region of the wave train in the Northern Hemisphere has happened. Members of the wave train are developed and their positions are adjusted in middle-high latitudes of the Northern Hemisphere. It is also clearly seen that circulation in the Northern Hemisphere is adjusting during the third and fourth five-day period.

Fig. 3c gives the sixth five-day averaged geopotential height difference at 300 hPa after the model is integrated. It is found that the phase of the difference center over the Pacific in the Southern Hemisphere is almost oppsite to that in Fig. 3b. What is important is that the tropical western Pacific is regarded as the source region of the wave trains not only in the Northern but also in the Southern Hemispheres. At that time, structure of the wave train in the Northern Hemisphere has been adjusted and it appears to be a similar pattern to that proposed by Nitta (1987) and Huang (1987).

The position and the phase of the difference centers in the Southern Hemisphere at 300 hPa in the second five-day averaged difference map appears to be rejuvenated as the model is integrated for the eighth five days (see Fig. 3d). The ray path of the wave train in the Southern Hemisphere as well as the phases basically agrees with each other in both maps. The important difference between these two maps is that the source region is shifted from equatorial central-eastern Pacific (Fig. 3a) to tropical western Pacific (Fig. 3d). In the Northern Hemisphere, it is clearly seen that a wave tarin exists, which is similar to the pattern suggested by Nitta (1987) and Huang (1987). By comparing Fig. 3d with 2a, the phases and positions of difference centers in the eighth five-day averaged difference map at 300 hPa are in basic agreement with those in the monthly averaged difference map at 300 hPa.

Of the above, it clearly indicated that first, the heat source in equatorial central-eastern Pacific may excite a wave train in each hemisphere in terms of the time scale within 10 days and their source region is situated in the heat source of equatorial central-eastern Pacific. It obviously reflects that these wave trains result from energy dispersion of the tropical disturbance forced by the equatorial heat source; second, the disturbance near the heat source, which is a member of the wave train on short time scale excited by the tropical heat source, results from local baroclinic response of tropical atmosphere to the heat source. Phases of the disturbance in the upper and lower troposphere are reverse. However, other members of the wave train far away from the heat source are equivalent-barotropic structure; third, main members of the wave train on time scale more than 10 days are developed and moved with basic flow and even change of reverse phase may take place during this period. These facts clearly indicate that with respect of short time scale, remote response of the atmosphere may result from energy dispersion of the heat source, but the energy dispersion does not play an important role in maintenance of atmospheric remote response and seems to be related to basic flow; fourth, it takes 35 days to complete the evolution and adjustment processes of atmospheric remote response in the winter hemisphere whereas in the summer hemisphere, it takes relatively longer. This phenomenon might be related to the structure of basic flow; fifth, the source region of the wave trains in both hemispheres shifts to tropical western Pacific although the positive SSTA over equatorial central-eastern Pacific still exists after the model is integrated for more than 10 days. This simulation shows that remote response in middle-high latitudes may be viewed as the result of Walker cell weakened by warm SST over equatorial central-eastern Pacific rather than direct forcing of anomalous SST over equatorial central-eastern Pacific. As a result, it causes anomalous convective activities resulting in exciting a wave train in both the Northern and Southern Hemispheres. Therefore, the main energy source of generating the wave trains on time scale less than 10 days is energy dispersion of disturbances forced by the heat source, and anomalous convective activities over tropical western Pacific dominates when the time scale greater than 10 days is considered, in which the main energy source region of wave trains in both hemispheres is tropical western Pacific. The above results is not only in agreement with the conclusion suggested by Branstator (1985), but also logically extended to the Southern Hemisphere.

V. DEVELOPMENT AND MAINTENANCE OF THE SHORT RANGE CLIMATIC OSCILLATIONS ON MONTHLY (SEASONAL) TIME SCALE

In the previous section, it has already been pointed out that development and maintenance of the short range climatic oscillation on monthly (seasonal) time scale is related to basic flow. Therefore, in order to investigate this problem, we have respectively calculated the barotropic conversion term of eddy kinetic energy and the conversion term from potential energy of disturbances to eddy kinetic energy. Assuming that short range climatological mean flow is a function of not only y but also x, the eddy kinetic energy equation describing the change of eddy kinetic energy is written as

$$\frac{\partial K_E}{\partial t}=CK_{BTX}+CK_{BTY}+CK_p, \qquad (1)$$

where

$$CK_{BTX}=\overline{-(u^{*2}-v^{*2})\frac{\partial u_b}{\partial x}}, \qquad (2)$$

$$CK_{BTY}=\overline{-u^*v^*\left(\frac{\partial u_b}{\partial y}+\frac{\partial v_b}{\partial x}\right)}$$

$$\simeq\overline{-u^*v^*\frac{\partial u_b}{\partial y}}, \qquad (3)$$

$$CK_p=\overline{\phi^*\left(\frac{\partial u^*}{\partial x}+\frac{\partial v^*}{\partial y}\right)}, \qquad (4)$$

where u_b and v_b represent the zonal and meridional components of basic flow, respectively; u^*, v^* and ϕ^* represent departures of u, v and ϕ from the normal case, that is, disturbed quantities. The first term is combined with the second terms in (1) as follows:

$$\left(\frac{\partial K_E}{\partial t}\right)_{BT}=\overline{E\cdot\nabla u_b}, \qquad (5)$$

where

$$E=-(u^{*2}-v^{*2},\ u^*v^*), \qquad (6)$$

E represents the horizontal component of EP flux. Eq. (5) gives the barotropic conversion term of eddy kinetic energy. Eq. (4) gives the conversion from potential energy of disturbances to eddy kinetic energy.

(1) *Maintenance of climatic oscillation in the monthly averaged difference map*

According to Eqs. (2) and (3), it is seen that barotropic conversion of eddy kinetic energy depends mainly on the zonal and meridional shear of the zonal basic flow, the meridional transport of disturbance momentum and the difference between zonal and meridional kinetic energy of disturbance (it reflects the difference between lengths of south-north and east-west axes, that is, horizontal structure of the disturbance). The conversion term of eddy kinetic energy formulated by (4) depends on the potential energy and divergence of disturbances.

Fig. 4 gives distribution of monthly averaged eddy kinetic energy conversions. The stippled regions with slopping lines and bars represent positive barotropic conversion of eddy kinetic energy and conversion from eddy potential energy to eddy kinetic energy, respectively.

The results show that the increase regions of barotropic conversion of eddy kinetic energy (decrease areas not shown) are situated in each disturbed member area of the wave train in both hemispheres, that is, large zonal and meridional shear areas of basic flow. However, the computed results also show that computed values from Eqs. (2) and (3) are of same magnitude. This result agrees with Simmons (1983).

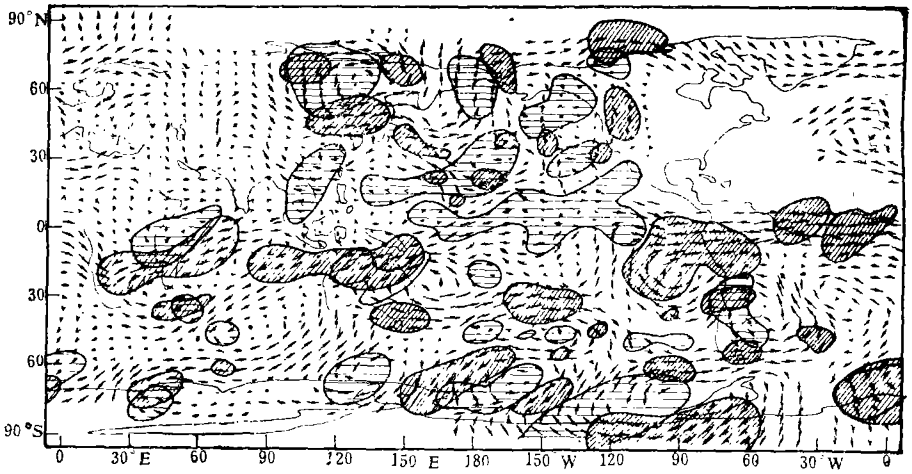

Fig. 4. Distribution of July mean eddy kinetic energy conversions from simulation. The stippled regions with slopping lines represents conversion from zonal kinetic energy to eddy kinetic energy; and the stippled regions with bars gives conversions from eddy potential energy to eddy kinetic energy.

Fig. 4 further indicates that barotropic conversion of eddy kinetic energy mainly takes place in the entrance of westerly jets to the north and west of the Xizang Plateau and the strongest shear region between westerly and easterly in the Southern Hemisphere. These regions just are location of members of wave trains in Southern and Northern Hemispheres. It is noteworthy that the narrow zone to the east of the heat source and along the equator is a positive barotropic conversion area of eddy kinetic energy and it is also a strongest westerly difference region to the east of the heat source. It implies that this region is a Kelvin wave response region to the east of the heat source. Therefore, Kelvin wave over the east of the equatorial heat source results from zonal kinetic energy converting to eddy kinetic energy. (The conversion is induced by barotropic instability of zonal flow). Results also show that the magnitude of eddy potential energy conversion term is comparable to that of barotropic conversion term. Furthermore, there is a one-to-one correspondence between the eddy potential energy conversion area and the member of the wave train in Southern and Northern Hemispheres and there is a larger conversion in the area where is closer to high latitudes.

The results described above clearly show that in the monthly averaged difference map, maintenance of two wave trains in Northern and Southern Hemispheres is directly related to barotropic conversion of eddy kinetic energy and the conversion from potential energy of disturbance to eddy kinetic energy. In other words, maintenance of short-range climatic oscillation on monthly time scale is not only related to barotropic instability of zonal flow, but also unstable development of disturbances (potential energy of disturbance converts to eddy kinetic energy). Comparing their magnitude, it is seen that both energy conversion terms play an important role in maintaining the wave trains. This result is not completely in agreement with Simmons (1983) who pointed out that oscillation on time scale more than one week was only related to barotropic instability. Therefore, gaining eddy kinetic energy from conversion of eddy potential energy for maintenance and development of disturbances is due to interaction between disturbances although vertical structure of short-range climatic oscillation on monthly time scale is equivelant-barotropic.

(2) *Effects of energy conversions on evolution processes of short-range climatic oscillations*

Fig. 5a represents distribution of the second five-day averaged energy conversion of eddy kinetic energy. From Fig. 2a it may be seen that a southeastward propagating wave train in the Southern Hemisphere and a wave train which propagates northwestward through near Japan then northward are formed on both sides of the equatorial heat source via energy dispersion. From Fig. 5a, it is seen that energy conversion from zonal kinetic energy and eddy potential energy to eddy kinetic energy has taken place in the location of the first two members of the wave train in the Southern Hemisphere. Similar conversions appear in the first two members of the wave train in the Northern Hemisphere. As a result, eddy kinetic energy is increased and disturbances of the wave trains are further developed. It is noteworthy that conversion from eddy potential energy to eddy kinetic energy exists in tropical western Pacific, South China and Indo-China Peninsula. It results in development of the northward propagating wave train over tropical western Pacific.

Fig. 5b represents distribution of the eighth five-day averaged conversion term of eddy kinetic energy, and indicates that large value areas of the conversion from zonal kinetic energy and eddy potential energy to eddy kinetic energy are just situated in the location of wave train members. Therefore, disturbances of the wave train gain eddy kinetic energy from zonal kinetic energy and eddy potential energy, then members of the wave train are maintained and developed. The result mentioned above clearly suggests that a disturbance gains eddy kinetic energy from zonal kinetic energy and eddy potential energy once it is formed by a localized forcing, and it disperses energy toward downstream and a new disturbance center is formed. If the new disturbance simultaneously gains eddy kinetic energy from zonal flow and eddy potential energy, the new disturbance is developed (otherwise, the new disturbance is suppressed, decayed and disappeared) and energy is continuously dispersed, and next new disturbance centers are generated. This dynamical process is continuously repeated and finally, a wave train is formed. Therefore, the formation procedure of a wave

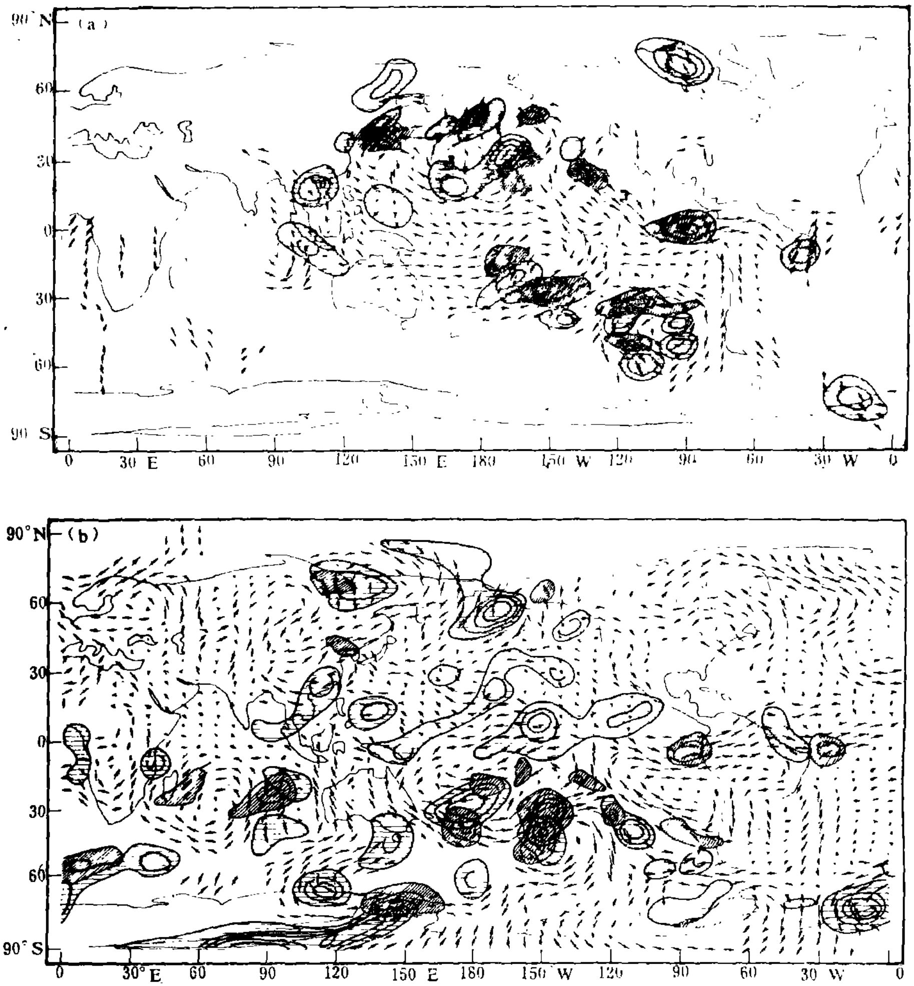

Fig. 5. Distribution of five-day averaged eddy kinetic energy conversions from simulation: (a) the second five-day average; and (b) the eighth five-day average. Others are same as in Fig. 4.

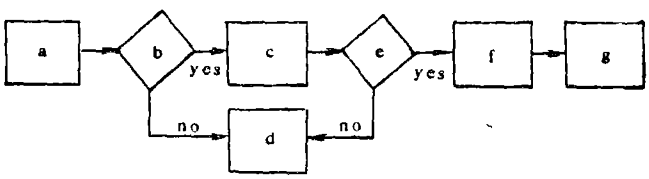

Fig. 6. Flow chart of the formation of a wave train.

a. response of the atmosphere to forcing and then form ation of a disturbance
b. conversions from zonal kinetic energy and eddy pttential energy to eddy kinetic energy
c. disturbance gains kinetic energy resulting in their developing, then energy is dispersed toward downstream and a new disturbance is formed
d. propagating disturbances are trapped
e. disturbances gain kinetic energy from zonal flow and eddy potential energy and they are developed
f. continuously disperse energy and next new disturbance is formed
g. a wave train is formed

train is schematically illustrated as shown in Fig.6.

From the flow chart mentioned above, it is clearly seen that only energy dispersion process is far too weak to account for propagation, development and maintenance of a wave train and their plausible explanation is a result of energy dispersion as well as interactions between eddies and zonal flow, and eddies. This result corrects the theory of energy dispersion proposed by Hoskins and Karoly (1981).

(3) *A numerical experiment of "switch off" SSTA over equatorial central-eastern Pacific*

In order to identify importance of energy conversions from zonal kinetic and eddy potential energy to eddy kinetic energy in the development and maintenance of the short

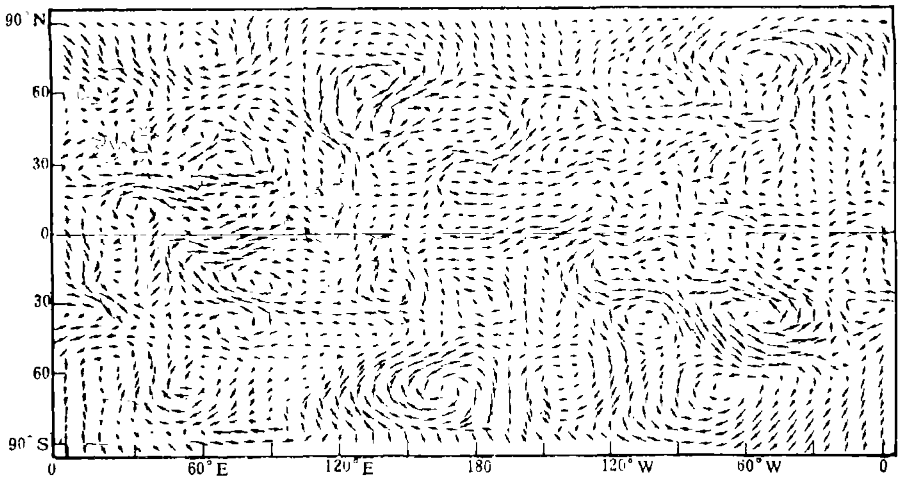

Fig. 7. The third five-day averaged difference flow from "switch off" experiment.

range climatic oscillation, the model with removal of SSTA over equatorial central-eastern Pacific, that is, recovery of normal mean SST field (same as SST field in Exp 1), is integrated for 15 days, after the model with SSTA in the same region is integrated for 40 days (e-folding time in the model is less than 10 days). This experiment is referred to as "switch off" experiment. Fig. 7 gives the third five-day averaged difference flow from "switch off" experiment. and clearly shows that anticyclonic difference circulations over south-east coast of China and west coast of North America and a cyclonic difference circulation over the northeast of China still exist in the Northern Hemisphere whereas in the Southern Hemisphere a wave train propagating toward southeast then turning northeastward is still maintained. This result further identifies that energy for the development and maintenance of short range climatic oscillation on monthly (seasonal) time scale mainly comes from interactions between eddies and zonal flow, and eddies. In other words, conversions from zonal kinetic energy and eddy potential energy to eddy kinetic energy are main energy source.

VI. CONCLUSIONS

According to the above simulation, the following conclusions can be drawn.

(1) Response of northern and southern atmosphere to SSTA over equatorial central-eastern Pacific is evident in northern summer. In the Northern Hemisphere, a wave train

that is similar to the teleconnection pattern suggested by Nitta (1987) and Huang (1987) is formed. The wave train has an influence on general atmospheric circulation and precipta-tion in East Asia and North America. Another wave train is also generated in the Southern Hemisphere, which affects not only atmospheric circulation there but also Asian summer monsoon via its effect on cross equatorial flow. Therefore, it is shown that SSTA over equatorial central-eastern Pacific may have an influence on atmospheric circulation in the Northern Hemisphere through short-range climatic oscillation in the Southern Hemisphere.

(2) In northern summer, the formation of two branches of wave trains on 10 day time scale in both hemispheres results from direct forcing of SSTA over equatorial central-eastern Pacific and the source region of wave trains is situated in the SSTA regions of equatorial central-eastern Pacific; when the time scale greater than 10 days is considered, the source region of wave trains is moved westward to tropical western Pacific although SSTA over equatorail central-eastern Pacific still exists. This fact shows that atmospheric remote response on monthly (seasonal) time scale in middle-high latitudes does not result from direct forcing of SSTA over equatorial central-eastern Pacific but arises from convection activity anomalies over tropical western Pacific, which is caused by SSTA over equatorial central-eastern Pacific. It is also shown that response of the atmosphere in middle-high latitudes of both hemispheres to the heating source over equatorial western Pacific is more sensitive than that to the heating source over equatorial central-eastern Pacific. These results not only confirm Branstator's (1985) conclusion but also can be logically extended to the Southern Hemisphere.

(3) In Northern summer, the process of producing the short-range climatic oscillation is not energy dispersion only and it arises as a result of energy dispersion as well as interactions between zonal flow and eddies, eddies. This result corrects the theory of energy dispersion suggested by Hoskins and Karoly (1981).

(4) Energy conversions from zonal kinetic energy and eddy potential energy to eddy kinetic energy play an important role in the development and maintenance of short-range climatic oscillation and are also an important energy source.

REFERENCES

Bjerknes, J. (1966), A possible response of the atmospheric Hadley circulation to equatorial anomalies of ocean temperature, *Tellus*, **18**: 820—829.

Blackmon, M. L., Lee, Y-H. and Wallace, J. M. (1984), Horizontal structure of 500 mb height fluctuation with long, medium and short periods, *J. Atmos. Sci.*, **41**: 961—979.

Branstator, G. (1985), Analysis of general circulation model sea surface temperature anomaly simulations using a linear model: I. Forced solutions, *J. Atmos. sci.*, **42**: 2225—2241.

Geister, J. E., Blackmon, M. L., Bates, G. T. and Munoz S. (1985), Sensitivity of January Climate response to the magnitude and position of equatorial Pacific sea surface temperature anomalies, *J. Atoms. Sci.*, **42**: 1037—1049.

Gill, A. E. (1980), Some simple solutions for heat-induced tropical circulation, *Quart. J. R. Met. Soc.*, **106**: 447—462.

Held, I. M. (1987), Barotropic model of the extratropical response to El Nino, *J. Atoms. Sci.*, **44**: 2576–3586.

Hendon, H. H. (1986), The time-mean flow and variability in a nonlinear model of the atmosphere with tropical diabatic forcing, *J. Atoms. Sci.*, **43**: 72—88.

Horel, J. D. and Wallace, J. M. (1981), Planetary-scale atmospheric phenomena associated with the Southern Oscillation, *Mon. Wea. Rev.*, **109**: 813—829.

Hoskins, B. J. and Karoly, D. J. (1981), The steady linear response of a spherical atmosphere to thermal and orographic forcing, *J. Atoms. Sci.*, **38**: 1179—1196.

Huang Ronghui and Li Weijing (1987), Influence of the heat source anomaly over the western tropical Pacific for the subtropical high over East Aisa, International Conference on the General Circulation of East Aisa, April 10—15, 1987, Chengdu, China, pp. 40—45.

Huang Ronghui and Wu Yutang (1988), The influence of the ENSO on the summer climatic change in China and its mechanism, *Adv. Atmos. Sci.*, (to be published).

Keshavamurty, R. N. (1982), Response of the atmosphere to sea surface temperature anomalies over the equatorial Pacific and the teleconnections of the sourthern oscillation, *J. Atoms. Sci.*, **39**: 1241—1259.

Lau, K. M. and Lim, H. (1984), On the dynamics of equatorial forcing of climate teleconnections, *J. Atoms Sci.*, **41**: 161—176.

Lau, N. C. (1981), A diagnostic study of recurrent meteorological anomalies appearing in a 15-year simulation with a GFDL general circulation model, *Mon. Wea. Rev.*, **109**: 2287—2311.

Lin Yuanbi and Sun Li (1987), Response of the atmosphere to central eastern equatorial Pacific sea surface temperature anomalies in July, *Scienita Met. Sinica*, 1987, No. 2, 1—13 (in Chinese).

McAvancy, B. J., Bourke, W. and Puri, K. (1978), A global spectral model for simulation of general circulation, *J. Atoms. Sci.*, **35**: 1557—1583.

Mo, K. C. and White, G. H. (1985), Teleconnections in the Southern Hemisphere, *Mon. Wea. Rev.*, **113**: 22—37.

Ni Yunqi, Qian Yongfu and Lin Yuanbi (1989), The effects of sea surface temperature over the Equatorial Western Pacific and the Indian Ocean on the Aisan summer monsoon, *Acta Met. Sinica* (to be published).

Ni Yunqi and Qian Yongfu (1989), The effects of sea surface temperature over the mid-latitude Western Pacific on the Asian summer monsoon, *Acta Met. Sinica* (to be published).

Nitta, T. (1987), Convective activities in the tropical western Pacific and their impact on the northern hemisphere summer circulation, International Conference on the General Circulation of East Aisa, April 10—15, 1987, Chengdu, China. pp. 121—126.

Ramage, C. S. (1975), Preliminary discussion of the meteorology of the 1972—1973 El Nino, *Bull. Amer. Meteor. Soc.*, **36**: 234—242.

Rasmusson, E. M. and Carpenter, T. H. (1982), Variations in tropical sea surface temperature and surface wind fields associated with the Southern Oscillation /El Nino, *Mon. Wea. Rev.*, **110**: 354—384.

Rowntree, P. R. (1972), The influence of tropical east Pacific Ocean temperature on the atmosphere. *Quart. J. Roy. Meteor. Soc.*, **98**: 290—321.

Rowntree, P. R. (1979), The effects of changes in ocean temperature on the Hemisphere, *Dyn. Atoms. Oceans*, **3**: 373—390.

Sardeshmukh, P. D. and Hoskins, B. J., (1985), Vorticity balance in the tropical during the 1982—1983 El Nino southern oscillation event, *Quart. J. Roy. Meteor. Soc.*, **111**: 261—278.

Sawyer, J. S. (1970), Observational characteristics of atmospheric fluctuations with a time scale of a month, *Quart. J. Roy. Meteor. Soc.*, **96**: 610—625.

Simmons, A. J., Wallace, J. M. and Branstator, G.W. (1983), Barotropic wave propagation and instability, and atmospheric teleconnection pattern, *J. Atoms. Sci.*, **40**: 1363—1392.

Van Loon, H. and Royers, J. C. (1978), The seasaw in winter temperature between Greenland and Northern Europe, Part I: General description, *Mon. Wea. Rev.*, **106**: 296—310.

Walker, G. T. and Bliss, E. W. (1932). World weather, *Mem. Roy. Meteor. Soc.*, **4**: 53—84.

Wallace, J. M. and Gutzler, L. S. (1981), Teleconnections in the geopotential height field during the Northern Hemisphere winter, *Mon. Wea. Rev.*, **109**: 784—812.

Webster R. J. (1981), Mechanism determining the atmospheric response to sea surface temperature anomalies, *J. Atoms. Sci.*, **38**: 554—571.

Webster, R. J. (1982), Seasonality in the local and remote atmospheric response to sea surface temperature anomalies, *J. Atoms. Sci.*, **41**: 41—52.